Journal of Electroanalytical Chemistry 662 (2011) 150–156

Contents lists available at ScienceDirect

Journal of Electroanalytical Chemistry

journal homepage: www.elsevier.com/locate/jelechem

Inhibition by CO of the corrosion of Fe, Ni, and their alloys in concentrated HCl solutions

Gema Cabello [a], Gary Funkhouser [b], Juanita Cassidy [b], José F. Marco [a], Claudio Gutiérrez [a], Angel Cuesta [a,*]

[a] Instituto de Química Física "Rocasolano", CSIC, C. Serrano 119, E-28006 Madrid, Spain
[b] Halliburton Energy Services, Inc., Duncan, OK 73536, USA

ARTICLE INFO

Article history:
Available online 27 May 2011

Keywords:
Corrosion inhibition
Adsorbed CO
Fe
Ni
Concentrated HCl
FTIRS

ABSTRACT

Inhibition by CO of the corrosion of Fe, Ni, and three alloys, containing either Fe and large amounts of Ni (Incoloy 825) or large amounts of Fe (Uniloy-420 and N80 steels) in solutions containing between 7.5% and 28% HCl was studied using potentiodynamic polarization curves, gravimetric tests, and FTIRS. In all cases, but Uniloy-420 in 28% HCl, a clear inhibition of corrosion in the presence of CO in the solution was shown by the gravimetric tests and from cyclic voltammetry, the inhibition being higher in the case of Ni and Ni-containing alloys. CO chemisorbed on Fe and/or Ni atoms present on the alloy surface was identified as the species responsible for corrosion inhibition. The inhibition of corrosion is higher in the cases of Ni and Incoloy 825.

1. Introduction

The adsorption of carbon monoxide on metal electrodes is a classical topic in interfacial electrochemistry, to which Andrzej Wieckowski has made significant contributions [1–7]. The interest in CO adsorption is mainly due to the detrimental role of adsorbed carbon monoxide in electrocatalysis, where it often acts as a poisoning intermediate that blocks active surface sites. This blocking effect, however, can be positive in other cases, for example in corrosion, a field that has also attracted Wieckowski's attention [8–14].

It is well known, from studies in UHV or at the gas–metal interface, that CO tends to chemisorb dissociatively on the transition metals at the left-hand side of the periodic table, and molecularly on those at the right-hand side. Although this is known to be an oversimplification, it is usually assumed that the dividing line between these two behaviors runs diagonally between Fe and Co, Tc and Ru, and W and Re [15]. This stimulated us some time ago to perform a study on the adsorption of CO on Fe and Co electrodes [16,17], which was extended to Ni electrodes. [18,19]. We could show that CO chemisorbs molecularly on all these metals in the pH range 3–14. Only CO adsorbed linearly (on-top CO, CO_L) could be found on Fe, while on Ni and Co CO was found to adsorb both on-top and at twofold bridge sites (CO_B), the ratio of the former to the latter increasing with decreasing pH (in the case of Co, the band corresponding to CO_B was very weak at pH 6.9, and undetectable at pH 3). Ten years later, the studies of CO adsorption on Fe [20], Co [21] and Ni [22–26] electrodes remain very scarce.

As a consequence of the strong chemisorption bond between CO and the surface atoms of the Fe, Co and Ni electrodes, surface oxidation or dissolution is impeded [16–19], a fact already reported by Uhlig in 1940 for stainless steels [27]. We report here a study of the inhibition by chemisorbed CO of the corrosion of Fe, Ni, Incoloy-825 (I825), Uniloy-420 (U420), and N80 carbon steel electrodes in very aggressive conditions: 7.5%, 15%, 20% and 28% HCl solutions, i.e., very acidic solutions with a high chloride concentration. Thanks to a simple new method recently developed by our group [28], we were able to use *in situ* external reflectance infrared spectra for studying the CO adsorption in these strongly acidic solutions using a fluorite window.

2. Experimental section

The working electrodes were disks of 12 mm in diameter, sanded with emery paper (600 grit) for electrochemical measurements and gravimetric tests, or polished with alumina down to a particle size of 0.05 μm for external reflectance infrared spectroscopy. In all the cases the samples were sonicated 2 min in acetone and then 5 min in Milli-Q water. Fe (99.998%) and Ni (99.99458%) were supplied by Alfa–Johnson Matthey. The alloys (I825, U420 and N80) were purchased from Metal Samples Co. The alloy compositions are shown in Table 1. Aqueous solutions containing 7.5%, 15%, 20% and 28% w/w HCl were used as electrolyte. Analytical grade reagents and Milli-Q water were used.

A Wenking analog potentiostat, in combination with a digital oscilloscope for signal recording, and a one-compartment

* Corresponding author.
E-mail address: a.cuesta@iqfr.csic.es (A. Cuesta).

1572-6657/$ - see front matter © 2011 Elsevier B.V. All rights reserved.
doi:10.1016/j.jelechem.2011.05.015

Table 1
Chemical composition (per cent mass) of I825, U420, and N80 alloys.

	C	Ni	Fe	Cr	Si	Cu	P	S	Mn	Mo	Ti	Al	Sn
I825	0.01	40.6	31.1	21.9	0.07	1.9	–	<0.001	0.44	2.8	1.1	0.1	–
U420	0.38	0.37	85.6	12.7	0.39	0.1	0.02	0.01	0.36	0.05	–	<0.02	0.01
N80	0.42	<0.02	97.4	0.012	0.19	0.04	0.13	0.14	1.66	0.016	0.001	<0.001	–

three-electrode cell were used for electrochemical measurements. The disk electrodes were set in a polypropylene holder with a Viton O-ring, with a brass screw pressed against the disk for providing electrical contact. A Pt wire and a home-made Ag/AgCl ($KCl_{sat.}$) electrode were used as the counter and reference electrodes, respectively. Blank measurements were performed in N_2-purged electrolyte (N50, Air Liquide). Measurements in CO-saturated solutions were performed after bubbling CO (N47, aluminum alloy cylinders, Air Liquide) for at least 20 min.

For the infrared measurements the disks were glued to a 5 mm length of Pyrex tubing, electrical contact to a copper cable being achieved with conductive epoxy resin. The measurements were performed with a home-made Pyrex cell containing a Pt wire and a home-made Ag/AgCl ($KCl_{sat.}$) electrode, that served as counter and reference electrodes, respectively. A CaF_2 prismatic window bevelled at 60°, protected by a thin (ca. 50 μm) commercial self-adhesive film (composed of atactic polypropylene and an acrylic adhesive and adhered to the surface of the prism facing the electrolyte, taking care not to leave any air bubble between the fluorite surface and the plastic film) [28], was attached at the bottom of the cell, which was placed on a home-made external reflectance accessory inserted in the sample chamber of a 1725-X FTIR Spectrometer from Perkin–Elmer, purged with CO_2– and H_2O–free air. The potential was controlled by a PAR potentiostat, Model 362, connected to a Synthesized Function Generator, Model DS345 from Stanford.

Reflectance spectra were recorded using *p*-polarized light, unless otherwise stated, and were calculated as $\frac{\Delta R}{R} = \frac{R_s}{R_{ref}} - 1$, where R_s and R_{ref} correspond to the single beam reflectance spectrum at the sample and reference potentials, respectively, each single spectrum consisting of 100 interferograms with a resolution of 8 cm^{-1}. A negative band indicates that a species present at the reference potential is consumed at the sample potential. Conversely, a positive band indicates that a new species, not present at the reference potential, is produced at the sample potential. A bipolar band indicates a Stark shift of a chemisorbed species present at both the reference and sample potentials.

Gravimetric tests were performed by immersing previously weighed disks of I825, U420 or N80 in air-saturated, N_2-purged, and CO-saturated 20% HCl. Mass losses were determined after 1, 2 and 3 days (I825), or after 1, 2 and 4 h (U420 and N80) of immersion in the above-mentioned solutions, and normalized by the surface area exposed to the solution. The results provided are the average of three measurements. Inhibition efficiency was calculated as $IE = \frac{\Delta m_{N_2} - \Delta m_{CO}}{\Delta m_{N_2}} \times 100$, where Δm_{N2} and Δm_{CO} are the area-normalized mass losses in N_2-purged solution and in CO-saturated solution, respectively, both after a given immersion time.

3. Results and discussion

Since all the alloys studied contain a large amount of iron, and, in the case of I825, also a large amount of nickel (see Table 1), knowledge of the interaction of CO with Fe and Ni was a prerequisite for the study of CO adsorption on the alloys of interest. Although the adsorption of CO on Fe and Ni electrodes has been studied previously [16–26], no study has been reported in the literature regarding the interaction of CO with these metals in the very aggressive conditions under which I825, U420 and N80 are often used.

3.1. Electrochemical measurements and gravimetric tests

Table 2 shows the values of the corrosion potential, E_{corr}, measured as the open circuit potential, for Fe, Ni, I825, U420 and N80. E_{corr} can also be measured as the potential at which the current crosses through zero in a potentiodynamic polarization curve at a slow scan rate. However, especially in the case of CO-saturated solutions, this value depends enormously on the electrode's history (as was to be expected, because E_{corr} is a kinetic, and not a thermodynamic, quantity), while the values of the open circuit potential were very reproducible (the standard deviation was usually ±5 mV, ±30 mV in the worst cases). As a general rule, E_{corr} shifts positively upon saturating the solution with CO, and, also as a general rule, the larger the shift the larger the corrosion inhibition found in subsequent potentiodynamic polarization and/or gravimetric experiments.

Figs. 1–3 show potentiodynamic polarization curves at 1 mV s^{-1} of Fe and Ni (Fig. 1), I825 and N80 (Fig. 2), and U420 (Fig. 3) in CO-free and CO-saturated concentrated hydrochloric acid solutions.

In the case of Fe and Ni (Fig. 1), only the potentiodynamic polarization curves in the most concentrated solution (28% HCl) are shown, since the results in the other three media were similar. In N_2-purged solution, no passivity region exists, and the corrosion rate increases exponentially at potentials between 50 and 100 mV above the potential at which the current crosses through zero in the first positive sweep. In CO-saturated solution, a reduction of the corrosion current below ca. −0.3 V is clearly observed in the case of Fe, while in the case of Ni a CO-induced inhibition of corrosion appears between ca. −0.3 and ca. −0.15 V.

In the case of I825 and N80 (Fig. 2) only the lowest and the highest concentrations used are shown. For I825, the potentiodynamic polarization curves in 7.5% HCl (Fig. 2A) are different from those in the other concentrations used. In N_2-purged 7.5% HCl solution, I825 shows an anodic peak, after which the current increases exponentially (but with a very high slope of 255 mV/decade), as typical of pitting corrosion after breakdown of the passive layer,

Table 2
E_{corr} (measured as the open circuit potential, in volts) of Ni, Fe, I825, N80 and U420 electrodes in N2-purged and CO-saturated HCl solutions.

	Ni		Fe		I825		N80		U420	
	N_2	CO	N_2	CO	N_2	CO	N_2	CO	N_2	CO
7.5% HCl	−0.328	−0.300	−0.435	−0.345	−0.209	−0.120	−0.410	−0.385	−0.467	−0.457
15% HCl	−0.332	−0.305	−0.440	−0.360	−0.230	−0.135	−0.366	−0.345	−0.445	−0.429
20% HCl	−0.356	−0.325	−0.463	−0.376	−0.245	−0.140	−0.383	−0.365	−0.447	−0.437
28% HCl	−0.370	−0.338	−0.402	−0.409	−0.265	−0.175	−0.390	−0.384	−0.423	−0.418

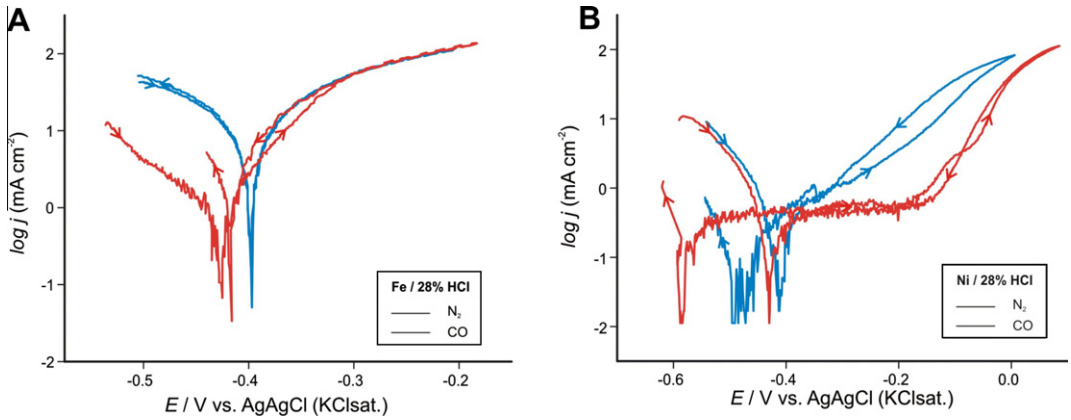

Fig. 1. Potentiodynamic polarization curves at 1 mV s^{-1} of Fe (A) and Ni (B) in 28% HCl solutions. The blue lines correspond to N_2-purged, deoxygenated solutions, while the red lines correspond to CO-saturated solutions. (For interpretation of the references to color in this figure legend, the reader is referred to the web version of this article.)

followed by a transpassivation peak. In the negative sweep the higher positive current observed suggests the occurrence of pitting corrosion, repassivation occurring around −0.1 V. In CO-saturated solution, there is again a CO-induced inhibition of corrosion preceding the peak, which is now clearly smaller than in the absence of CO. At higher HCl concentrations the behavior is similar to that observed in 28% HCl (Fig. 2B). In this case, both in N_2-purged and in CO-saturated solutions there is no peak. However, a CO-induced inhibition of corrosion appears in CO-saturated solutions, the current increasing exponentially at more positive potentials, most likely because the protection provided by chemisorbed CO disappears upon its oxidation. In the negative sweep the CO induced inhibition of corrosion reappears, suggesting that CO readsorbs on the surface of the I825 alloy.

For N80, the potentiodynamic polarization curves show a gradual change from that in 7.5% HCl (Fig. 2C) to that in 28% HCl (Fig. 2D), with a narrow region of CO-induced inhibition of corrosion, whose width decreases with increasing HCl concentration and disappears in 28% HCl.

In the case of U420 (Fig. 3), the potentiodynamic polarization curves depended strongly on the HCl concentration. At the highest concentration used (28% HCl) the potentiodynamic polarization curve was practically unaffected by CO. At the lowest concentration, 7.5% HCl, a CO-induced inhibition of corrosion appeared. At 15% and 20% HCl the behavior is intermediate between those in 7.5% HCl and in 28% HCl. There are three interesting features worth noting in the potentiodynamic polarization curves of U420 in Fig. 3A, B and D, although at this moment we do not have an

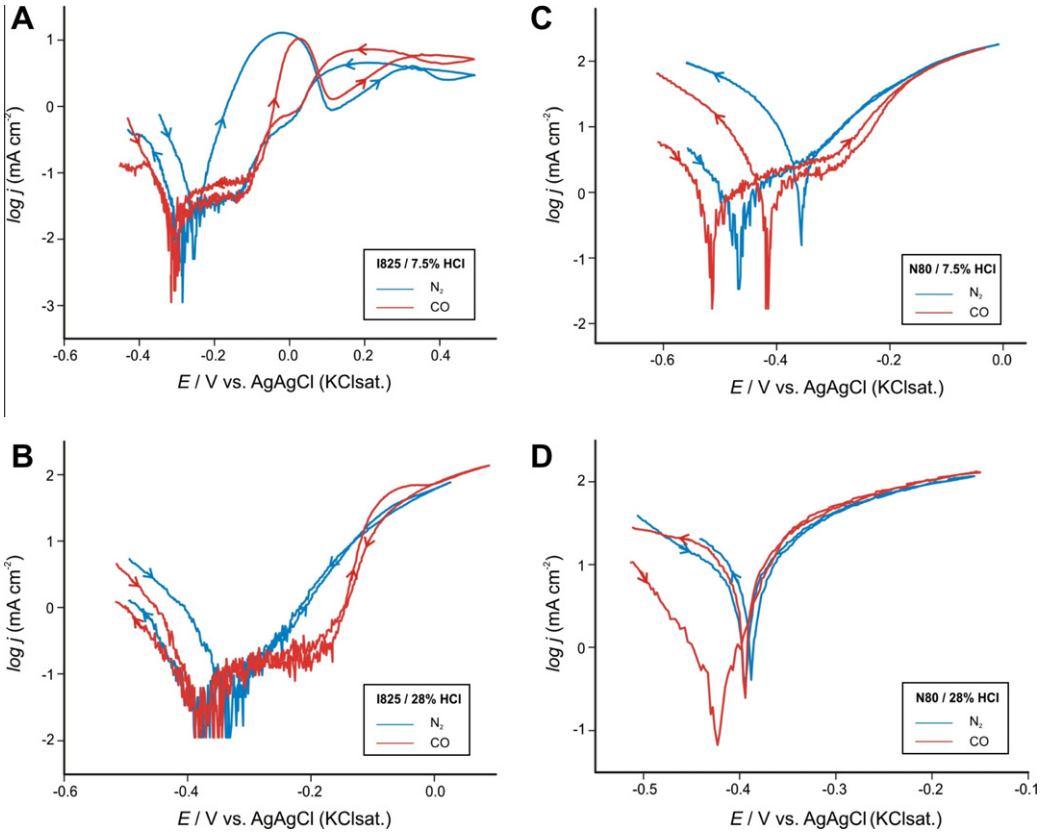

Fig. 2. Potentiodynamic polarization curves at 1 mV s^{-1} of I825 (A and B) and N80 (C and D) in 7.5% (A and C) and 28% HCl (B and D) solutions. The blue lines correspond to N_2-purged, deoxygenated solutions, while the red lines correspond to CO-saturated solutions. (For interpretation of the references to color in this figure legend, the reader is referred to the web version of this article.)

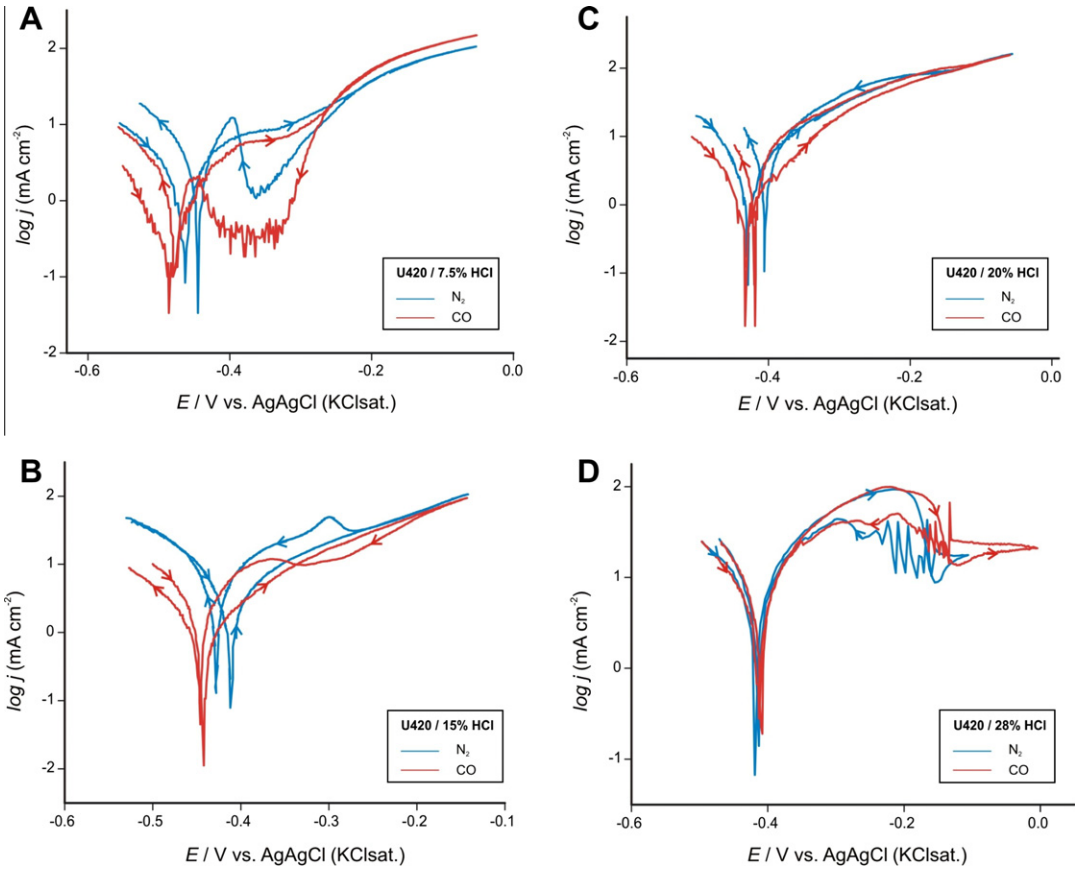

Fig. 3. Potentiodynamic polarization curves at 1 mV s^{-1} of U420 in 7.5% (A), 15% (B), 20% (C) and 28% HCl (D) solutions. The blue lines correspond to N_2-purged, deoxygenated solutions, while the red lines correspond to CO-saturated solutions. (For interpretation of the references to color in this figure legend, the reader is referred to the web version of this article.)

explanation for all of them: (i) the enhanced repassivation in 7.5% HCl (Fig. 3A) at $E < -0.2$ V in CO-saturated solution in the negative sweep, as compared with the N_2-purged solution; (ii) the anodic peak at around −0.3 V in the negative sweep in N_2-purged 20% HCl (Fig. 3B); and (iii) the oscillatory behavior slightly above −0.2 V during the negative sweep both in N_2-purged and CO-saturated 28% HCl (Fig. 3D). This oscillatory behavior has been attributed to metastable pitting [29–31], during which local nucleation, growth and repassivation of pits occurs. The process is observed in the negative sweep because it requires the previous formation of a passive film.

In all the cases but N80 and U420 in 28% HCl, a clear corrosion inhibition is observed upon saturating the solutions with CO, as deduced from the current decrease. The inhibition of corrosion is accompanied in all cases by a clear decrease of the hydrogen evolution current at the negative limit of the potential scan, suggesting that strong chemisorption of CO blocks some of the surface atoms, as confirmed by infrared spectroscopy (see below). The inhibition of corrosion by CO must be, hence, due to the suppression of the cathodic reaction (hydrogen evolution in the absence of oxygen).

In addition to this blocking effect, CO is a reducing agent because it can be oxidized to CO_2 on sufficiently active surfaces. Obviously this reducing action of CO will obtain only as far as there is CO in solution for replacing the oxidized CO. As can be deduced from our previous work on CO adsorption on Fe [16] and Ni [18,19], CO is oxidized on Fe at lower potentials than on Ni, indicative of a higher activity of Fe towards CO oxidation, as confirmed by the absence of a flat, nearly constant current region in the potentiodynamic polarization curves of Fe in the concentrated HCl solutions used here. In any case, CO oxidation is not expected to contribute substantially to the corrosion current under open circuit conditions.

We attempted to quantify the degree of corrosion inhibition by determining i_{corr} in CO-free and CO-containing solutions by extrapolating the current in the exponential region of the potentiodynamic polarization curves down to the potential at which the current crosses through zero in the positive sweep, but this is only possible in the cases where the potentiodynamic polarization curves show Tafel-like behavior, like in Fig. 1A, and, in addition, the value of the potential at which the current crosses through zero in the positive sweep is extremely sensitive to the electrode's history. We also attempted to determine i_{corr} by the *polarization resistance* method, that consists of measuring the current flowing through the interface in a small potential interval (10–20 mV) around the corrosion potential, the slope of the (usually linear) potential vs. current sweep being directly proportional to the corrosion rate at the corrosion potential, but we found again a large irreproducibility and a strong dependence on the electrode's history of the absolute values of the corrosion rate (not surprisingly, since corroding systems are far from equilibrium). For these reasons, we decided to perform gravimetric corrosion tests which, contrary to i_{corr} determined by electrochemical methods, corresponding to the corrosion rate at the moment at which the measurement is performed, yield a value of the corrosion rate averaged over longer periods. The result of the gravimetric tests, that were performed only for I825, N80 and U420 in 20% HCl, are shown in Fig. 4.

Fig. 4A–C shows the mass loss as a function of time in air-saturated (black), N2-purged (blue) and CO-saturated (red) solutions.

In the case of I825 (Fig. 4A) and U420 (Fig. 4C), removal of oxygen from the solution by N2-bubbling results in a decrease in the mass loss, while in the case of N80 the mass loss is higher after deoxygenating the solution, suggesting that, in the latter case, the presence of oxygen favors the formation of a passivating oxide layer.

The gravimetric tests confirm the conclusion reached from the potentiodynamic polarization curves that CO inhibits the corrosion of all the materials studied, although the inhibition is clearly higher in I825 (Fig. 4A and D) than in the other two alloys. In addition, in the case of I825 in the presence of CO, most of the mass loss due to corrosion occurs during the first 24 h, additional mass losses after 2 or 3 days of immersion in 20% HCl being undetectable (Fig. 4A, red line). As a consequence, in the case of I825 the efficiency of CO as a corrosion inhibitor increases from 57% after 1 day of immersion in HCl 20% to 83% after 3 days of immersion (Fig. 4D). High inhibition efficiencies (above 70%) are also reached with N80 (Fig. 4E), although in this case, after reaching a maximum, the efficiency decreases continuously with time. In the case of U420 (Fig. 4F), although the inhibition efficiency is initially high (more than 55%), it decreases continuously with time, and after 4 days is below 25%.

3.2. FTIRS

In order to confirm that chemisorbed CO is the species responsible for the inhibition of corrosion observed in CO-containing solutions, we performed a FTIRS study.

Fig. 5 shows FTIR spectra of Ni (red line), iron (green line), polished I825 (solid blue line), and passivated I825 (dashed blue line) in CO-saturated 7.5% HCl. The black line in Fig. 5 corresponds to the sum of the FTIR spectra of CO adsorbed on Ni and on Fe. At higher HCl concentrations, similar spectra were observed, but they were often disturbed by the presence of small hydrogen bubbles, formed at the negative potentials used as reference.

In the case of Ni, we could observe some differences with the previously reported spectra [18,19]. Although the spectra show bipolar bands corresponding to linear CO_L between 2053 and 2072 cm^{-1} and CO_B around 1970 cm^{-1}, the intensity of the latter decreasing with decreasing pH, as reported earlier, we could observe an additional band at 2043 cm^{-1}, whose frequency does not change with the electrode potential. In addition, this band can also be observed in spectra recorded using *s*-polarized light (see Fig. S1 in the Supplementary Information), indicating that this band must correspond to a species in solution, and not to an adsorbed species. Its frequency [32–34] allows us to assign this band to $Ni(CO)_4$ in solution. It should be noted that no $Ni(CO)_4$ could be detected by us in our previous study of CO adsorption on Ni electrodes at pH 3–14. Accordingly, and taking into account the low solubility of $Ni(CO)_4$ in aqueous solutions, we suggest that its formation must be due to reaction of CO with Ni^{2+} present in the solution as a product of corrosion.

The spectra of CO chemisorbed on Fe electrodes are similar to those previously reported by us [16], showing a single bipolar band between 2003 and 2020 cm^{-1}, attributed to CO_L. As expected, and following the tendency reported by us previously, the band of CO_L on Fe appears at higher frequencies as the pH decreases, due to the positive shift of the accessible potential window.

On polished I825 electrodes (solid blue line in Fig. 5) the only clearly observable band is that corresponding to CO_L adsorbed on Ni (between 2052 and 2068 cm^{-1}). No band corresponding to CO_B on Ni emerged above the noise level. The absence of bands corresponding to CO_L on Fe is remarkable, taking into account the high Fe content of the alloy. Two explanations are plausible: either (i) the iron present in the alloy has electronic properties different from those of pure iron, not binding CO, or (ii) there has been a surface segregation phenomenon, depleting iron from the alloy's surface and enriching it with nickel. The latter hypothesis is supported by the bands observed on an I825 sample that had been left immersed in 7.5% HCl overnight (*passivated* I825). Under these conditions, the spectrum (dashed blue line in Fig. 5) shows a small band corresponding to CO_L on Fe in addition to the band corresponding to CO_L adsorbed on Ni also observed with polished I825. The assignment of the small bipolar band between 2020 and 2035 cm^{-1} to CO_L on Fe is confirmed by the close resemblance between the spectrum of CO adsorbed on *passivated* I825 and the spectrum resulting of adding the spectra of CO adsorbed on Ni

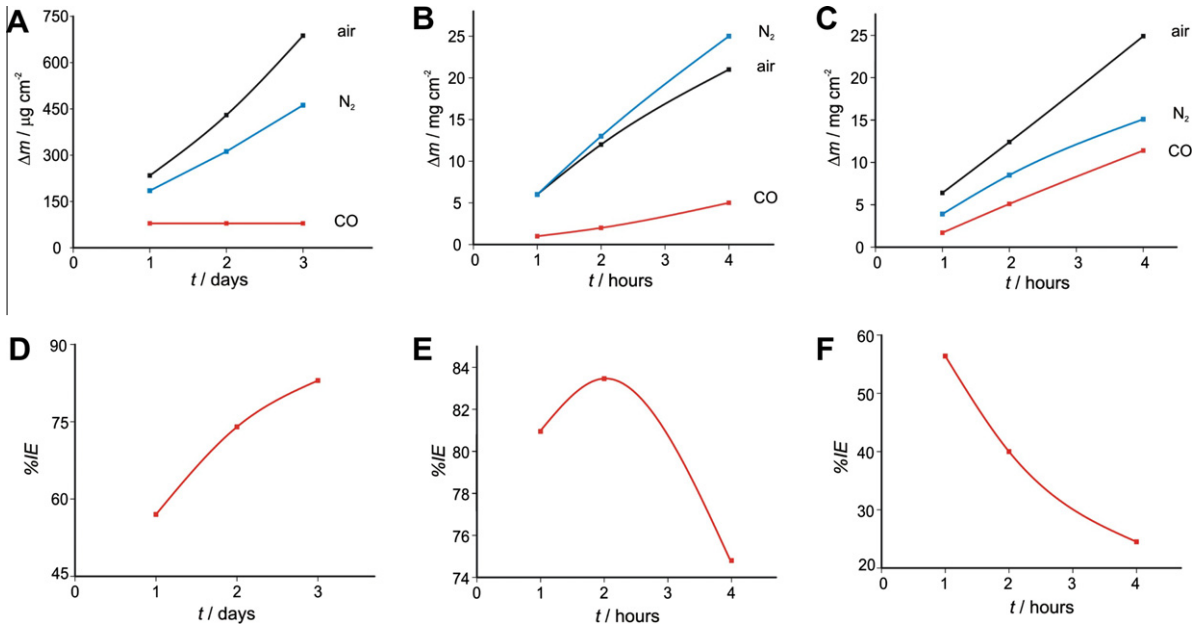

Fig. 4. Mass loss of I825 (A), N80 (B) and U420 (C) as a function of immersion time in 20% HCl. Black, blue and red lines correspond to experiments performed, in air-, N_2 and CO-saturated solutions, respectively. The corresponding inhibition efficiencies in CO-saturated solutions as compared to N_2-purged solutions are shown in D, E and F, respectively. (For interpretation of the references to color in this figure legend, the reader is referred to the web version of this article.)

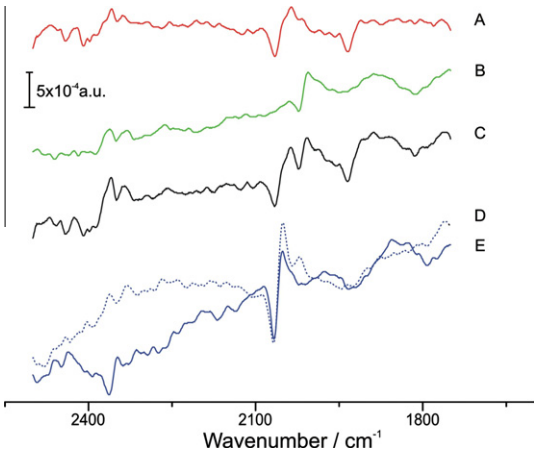

Fig. 5. SW-FTIR spectra of (A) Ni (E_{ref} = 0.02, E_s = −0.25), (B) Fe (E_{ref} = −0.35, E_s = −0.4) and (D, E) I825 (E_{ref} = −0.05, E_s = −0.32) electrodes in 7.5% HCl. The solid blue line (E) corresponds to a polished I825 electrode, and the dashed blue line (D) to a I825 sample that was left immersed overnight in 7.5% HCl. The black line (C) is the sum of the red and green lines. (For interpretation of the references to color in this figure legend, the reader is referred to the web version of this article.)

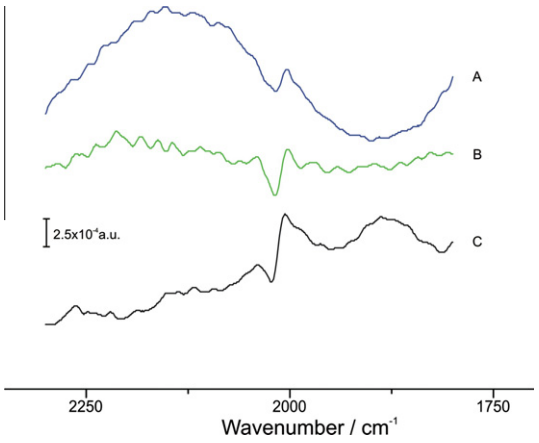

Fig. 6. SW-FTIR spectra of (A) U420 (E_{ref} = −0.28, E_s = −0.4), (B) N80 (E_{ref} = −0.32, E_s = −0.4), and (C) Fe (E_{ref} = −0.35, E_s = −0.4) electrodes in 0.01 M HCl.

and of CO adsorbed on Fe (black line, Fig. 5). Note that the small difference in the frequencies at which the bipolar bands appear in the spectrum of CO adsorbed on I825 and in the spectra of CO adsorbed on Ni and Fe are due to the differences in the potentials at which the spectra were recorded, typically more negative in the case of Ni and Fe due to their lower corrosion resistance, as compared to I825.

The presence of the band corresponding to CO_L on Fe in the spectrum of CO adsorbed on *passivated* I825 suggests that iron on the alloy surface behaves similarly to pure iron and, consequently, leads to the conclusion that the absence of this band on polished I825 is most likely due to the very small amount of Fe present on the surface, the concentration of Fe on the alloy's surface increasing after the *passivation* treatment. This is in disagreement with XP spectra of I825 recorded before and after the treatment with concentrated HCl (see Fig. S2 in the Supplementary Information), which show no significant variation of the relative amount of Fe and Ni present on the alloy's surface. XP spectra show a clear increase of the amount of Mo present on the surface of the alloy, although CO does not chemisorb on Mo, and, hence, no contribution of this metal to the corrosion inhibition by CO is to be expected, as confirmed by the FTIR spectra in Fig. 5. It must be noted, however, that FTIRS probes the very top atomic surface layer, while XPS probes a region several layers deep, 3 nm average. Furthermore, XPS is an *ex situ* technique and, accordingly, the surface composition obtained from it does not necessarily coincide with the composition present when the alloy is in contact with a concentrated HCl solution.

On I825, we did not find any evidence suggesting the presence on the surface of CO_B bonded to a Ni and a Fe atom, or the presence of metal carbonyls in solution.

Fig. 6 shows FTIR spectra of N80 and U420 in CO-saturated 10^{-2} M HCl solutions. In these cases, the spectra had to be recorded with a lower HCl concentration due to the large amount of H_2 bubbles formed at the reference potential. Fig. 4 also includes the FTIR spectrum of Fe in the same solution, for the sake of comparison. The spectra of U420 and N80 (blue and green lines, respectively, in Fig. 4) in CO-containing solutions are similar to those of Fe, showing a single band attributed to CO_L on Fe, as was to be expected due to the high iron content of these two alloys (see Table 1).

4. Conclusions

Corrosion of Fe, Ni, and alloys containing large amounts of Fe and Ni (I825) or Fe (U420, N80) is inhibited in CO-containing solutions. FTIRS shows that the inhibition of corrosion is due to the presence on the surface of strongly chemisorbed carbon monoxide blocking the surface and protecting it against corrosion, even in strongly acidic solutions with high chloride concentrations. On Fe electrodes CO adsorbs as CO_L, while on Ni electrodes both CO_L and CO_B are detected, the amount of the latter decreasing with decreasing pH, in agreement with previous reports. On I825, an alloy containing ca. 41% Ni and ca. 31% Fe, only CO_L on Ni can be detected on the as-polished surface, while both CO_L on Ni and CO_L on Fe are detected if the sample was left overnight in 7.5% HCl. The band corresponding to CO_B on Ni is absent in both cases. U420 and N80 behave nearly identically to pure Fe with respect to CO adsorption.

Acknowledgements

We thank Prof. Mª Cruz Alonso and Dr. Francisco J. Recio for useful discussions, and Mr. Nicomedes Sanrromán for helping us to design our spectroelectrochemical cell.

Appendix A. Supplementary material

Supplementary data associated with this article can be found, in the online version, at doi:10.1016/j.jelechem.2011.05.015.

References

[1] L.W.H. Leung, A. Wieckowski, M.J. Weaver, J. Phys. Chem. 92 (1988) 6985–6990.
[2] R.X. Liu et al., J. Phys. Chem. B 104 (2000) 3518–3531.
[3] Y.Y. Tong, H.S. Kim, P.K. Babu, P. Waszczuk, A. Wieckowski, E. Oldfield, J. Am. Chem. Soc. 124 (2002) 468–473.
[4] Y.Y. Tong, C. Rice, A. Wieckowski, E. Oldfield, J. Am. Chem. Soc. 122 (2000) 1123–1129.
[5] P. Waszczuk, G.Q. Lu, A. Wieckowski, C. Lu, C. Rice, R.I. Masel, Electrochim. Acta 47 (2002) 3637–3652.
[6] P. Waszczuk, A. Wieckowski, P. Zelenay, S. Gottesfeld, C. Coutanceau, J.M. Leger, C. Lamy, J. Electroanal. Chem. 511 (2001) 55–64.
[7] M.J. Weaver, S.C. Chang, L.W.H. Leung, X. Jiang, M. Rubel, M. Szklarczyk, D. Zurawski, A. Wieckowski, J. Electroanal. Chem. 327 (1992) 247–260.
[8] A. Kolics, J.C. Polkinghorne, A.E. Thomas, A. Wieckowski, Chem. Mater. 10 (1998) 812–824.
[9] A. Kolics, J.C. Polkinghorne, A. Wieckowski, Electrochim. Acta 43 (1998) 2605–2618.

[10] A. Kolics, P. Waszczuk, L. Gancs, Z. Nemeth, A. Wieckowski, Electrochem. Solid State Lett. 3 (2000) 369–372.
[11] A. Kolics, A.S. Besing, P. Baradlai, R. Haasch, A. Wieckowski, J. Electrochem. Soc. 148 (2001) B251–B259.
[12] A. Kolics, A.S. Besing, A. Wieckowski, J. Electrochem. Soc. 148 (2001) B322–B331.
[13] L. Gancs, A.S. Besing, R. Bujak, A. Kolics, Z. Nemeth, A. Wieckowski, Electrochem. Solid State Lett. 5 (2002) B16–B19.
[14] A. Kolics, A.S. Besing, P. Baradlai, A. Wieckowski, J. Electrochem. Soc. 150 (2003) B512–B516.
[15] J.P. Muscat, D.M. Newns, Prog. Surf. Sci. 9 (1978) 1–43.
[16] A. Cuesta, C. Gutierrez, J. Phys. Chem. 100 (1996) 12600–12608.
[17] A. Cuesta, C. Gutierrez, Langmuir 14 (1998) 3390–3396.
[18] A. Cuesta, C. Gutierrez, J. Phys. Chem. B 101 (1997) 9287–9291.
[19] A. Cuesta, C. Gutierrez, Langmuir 14 (1998) 3397–3404.
[20] S.-J. Huo, J.-Y. Wang, J.-L. Yao, W.-B. Cai, Anal. Chem. 82 (2010) 5117–5124.
[21] Q.-S. Chen, S.-G. Sun, J.-W. Yan, J.-T. Li, Z.-Y. Zhou, Langmuir 22 (2006) 10575–10583.
[22] Y. Hori, O. Koga, A. Aramata, M. Enyo, Bull. Chem. Soc. Jpn. 65 (1992) 3008–3010.
[23] M. Zhao, K. Wang, D.A. Scherson, J. Phys. Chem. 97 (1993) 4488–4490.
[24] H.-C. Wang, S.-G. Sun, J.-W. Yan, H.-Z. Yang, Z.-Y. Zhou, J. Phys. Chem. B 109 (2005) 4309–4316.
[25] S.-J. Huo, X.-K. Xue, Yan, Q.-X. Li, M. Ma, W.-B. Cai, Q.-J. Xu, M. Osawa, J. Phys. Chem. B 110 (2006) 4162–4169.
[26] J.-Y. Wang, B. Peng, H.-N. Xie, W.-B. Cai, Electrochim. Acta 54 (2009) 1834–1841.
[27] H.H. Uhlig, Ind. Eng. Chem. 32 (1940) 1490–1494.
[28] G. Cabello, A. Cuesta, C. Gutiérrez, Electrochem. Commun. 11 (2009) 616–618.
[29] Y. Tang, Y. Zuo, Mater. Chem. Phys. 88 (2004) 221–226.
[30] Y.M. Tang, Y. Zuo, X.H. Zhao, Corrosion Sci. 50 (2008) 989–994.
[31] H. Wang, J. Xie, K.P. Yan, M. Duan, Y. Zuo, Corrosion Sci. 51 (2009) 181–185.
[32] L.H. Jones, J. Chem. Phys. 23 (1955) 2448.
[33] L.H. Jones, Spectrochim. Acta 19 (1963) 1899–1904.
[34] P.L. Prasad, S. Singh, J. Chem. Phys. 67 (1977) 4384–4397.